Dielectric-constant anomaly near the consolute point of a binary mixture: Nitrobenzene-isooctane

M. Merabet and T. K. Bose
Département de Physique, Université du Québec à Trois-Rivières, Trois-Rivières, Québec, Canada G9A 5H7
(Received 2 December 1980; revised manuscript received 11 June 1981)

The static dielectric permittivity of a nitrobenzene-isooctane mixture shows, along its critical isochore, a 0.3% deviation from normal behavior at a temperature of 5×10^{-3} K above T_c. Near the consolute point, no gravity effects resulting from composition gradients are detected. A free fit of the critical exponent θ yields a value of 0.855 ± 0.035, in good agreement with the theoretical values.

I. INTRODUCTION

Recent experimental and theoretical developments on critical phenomena have created substantial interest in liquid-liquid transitions.[1] In this work, we investigate the behavior of the static permittivity ϵ of a polar-nonpolar liquid mixture near the consolute point, when the latter is approached along the critical isochore.

The experimental situation in this domain was until recently rather confusing. Conflicting results have been reported on the behavior of $\epsilon(T)$ near the critical temperature T_c of similar binary mixtures in most cases nitrobenzene-alkanes mixtures. A sharp increase of ϵ for temperatures very close to T_c was observed by some authors[2–5]; while others[6–9] have obtained a smooth behavior. The disagreement as pointed out by Thoen *et al.*[10] can be related to the presence of ionic impurities. They found[10] that the ionic conductivity combined with the large composition fluctuations near the critical point give rise to a Maxwell-Wagner dispersion where the high-frequency limit f_{MW} is the lower bound from which the values of ϵ represent the real static permittivity. Then, results obtained at frequencies higher than f_{MW} can be compared to the theoretical predictions which will be presented in Sec. II.

In this paper, we report very-high-precision measurements of the static permittivity ϵ of a critical nitrobenzene-isooctane mixture as a function of temperature T, frequency f, and height h; focusing our attention on three items: low-frequency dispersion, nonexistence of composition gradients in the mixture near T_c, and finally the direct determination of the critical exponent θ of the static permittivity.

We chose this system because of its convenient critical temperature (302.2 K) and appreciable value of ϵ at that temperature (10.28), and because its critical behavior, which has been the subject of some studies,[3,8,9] is not conclusively known.

II. THEORY

When the critical point of a pure fluid or of a binary liquid mixture is approached along the critical isochore, all of the recent theories predict for the static permittivity ϵ near the critical temperature T_c, a leading behavior of the form:

$$\epsilon\simeq\epsilon_c+At^{\theta}\,, \tag{1}$$

where ϵ_c is the static permittivity at T_c, $t=(T-T_c)/T_c$ is the reduced temperature, and $\theta=1-\alpha$. The critical exponent α describes the singularity of the specific heat. Although these theories give the same predictions, they are quite different in their approaches.

The theory of Stell and Hoye[11] is specific to the critical behavior of ϵ of a simple nonpolar fluid. The Clausius-Mossotti function is expanded in powers of the polarizability and the authors[11] show that the lowest-order term in the expansion is closely related to the internal energy. If higher-order terms are neglected, the static permittivity should show the singularity of the internal energy.

Mistura[12] uses thermodynamic arguments and the smoothness postulate to relate also the singular part of the static permittivity to that of the internal energy. The singular part of the internal energy is characterized along the same critical path by

the critical exponent $1-\alpha$.

The theory of Goulon *et al.*[13] is a phenomenological analysis of the critical behavior of ϵ of binary liquid mixtures. The authors[13] combine the droplet model of Oxtoby and Metiu[14,15] which provides a physical picture of the microscopic nature of systems in the critical region, with the electrostatic models of Wagner[16] and of Onsager-Böttcher.[17] For both electrostatic models, the same asymptotic behavior of ϵ is derived. The expression for ϵ is identical to that of Eq. (1).

Recently, Sengers *et al.*[18] obtained a functional form for the static permittivity near the critical point that includes correction to scaling terms.[19] They apply the critical-point universality to the thermodynamic behavior of fluids and mixtures in the presence of an electric field. They found that along the critical isochore and for temperatures above the critical temperature T_c, the behavior of the static permittivity ϵ can be expressed as

$$\epsilon \simeq A_0 + A_1 t^{\theta} + B_1 t + C_1 t^{\theta+\Delta} , \qquad (2)$$

where Δ with a numerical value of 0.50 Ref. 20 is the correction to scaling exponent. The critical exponent θ is defined as in Eq. (1), i.e., $\theta = 1-\alpha$.

III. EXPERIMENTAL

The experimental study of the critical behavior of the static permittivity of a binary mixture along the critical isochore is difficult because of the weak $1-\alpha$ expected singularity. Such study requires precise temperature control and very high-precision permittivity measurements. We have already performed permittivity measurements with such precision in our laboratory to study molecular interactions in gases not far from the critical point.[21]

The present experiment consists in measuring the static permittivity of a critical nitrobenzene-isooctane mixture as a function of temperature at several frequencies between 0.1 and 100 kHz and at different heights in the sample. Details about the apparatus used and the experimental procedure are given below.

A. Apparatus used

The measuring cell (Fig. 1), is composed of an inner cylinder of 7.5-mm radius and 12 circular plates, each having an inner radius of 8.5-mm and 1-mm thickness. The cylinder and the plates are made from 316 stainless steel. The plates are insulated from each other by means of a thin Mylar sheet of 0.2-mm thickness. Each of the outside circular plates has an independent electrical connection. The 12 vertical capacitors thus assembled enable us to measure ϵ in function of height as well as for the whole system. When measuring a particular capacitor at a given height, all other circular plates are connected to the ground, thus acting as guarded electrodes.

The arrangement of the capacitors covers a 14-mm region in the middle of the sample cell. Capacities are measured with a General Radio three-terminal transformer bridge (model G. R. 1621). An advantage of this bridge is that coaxial cables do not add to the measured capacity.

The temperature of the sample cell is controlled to 0.3 mK per eight hours by means of a HAAKE thermo-regulator (model FE) and a TRONAC precision controller bath (model 40). Water in the bath is well stirred by a double downward pushing propeller so that no temperature gradients in the region where the sample cell is immersed, are detected. The temperature is measured using a quartz thermometer (model H. P. 2801A), which had recently been calibrated by the manufacturer with respect to a standard (N. B. S. certified) plati-

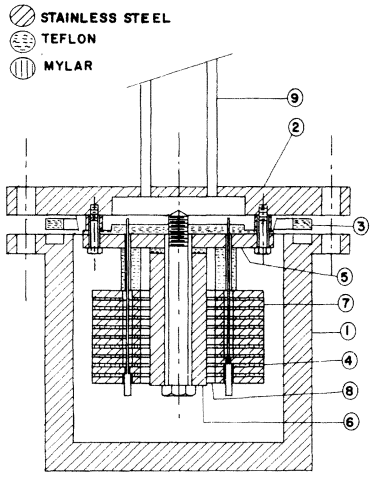

FIG. 1. Schematic diagram of the measuring cell. Legend: 1=sample container; 2=cover with 8 screws; 3=0 ring (Teflon); 4=capacitor array; 5=insulating holder; 6=low-electrode inner cylinder with 7.5-mm radius; 7=high-electrode circular plate of 1-mm thickness and inner radius of 8.5 mm. There are 12 circular plates insulated from each other by means of a thin Mylar sheet of 0.2-mm thickness; 8=measuring space between electrodes; 9=electrical outlets.

num resistance thermometer to 1 mK. The precision of the temperature measurements is 0.1 mK.

B. Experimental procedure

Nitrobenzene (Fisher S. C. certified A. C. S.) was first dried over calcium chloride, then over phosphorus pentoxide, and finally distilled two times under dry nitrogen at reduced pressure. At a temperature of 298 K, the final product has a static permittivity of 34.80 and a specific conductivity of 8.2×10^{-9} mho cm^{-1}. Isooctane (Fisher S. C. certified 99 mol. % pure) was distilled under dry nitrogen at atmospheric pressure. The purified material has a static permittivity of 1.921 at 298 K. For both components, the measured values of the static permittivity and of the specific conductivity compare well with the accepted values.[22]

The critical composition ($X_c=51.7$ wt. % nitrobenzene) and the critical temperature ($T_c=302.20\pm0.04$ K) are determined visually, in agreement with the values reported by Debye and Kleboth[23] ($X_c=51.7$ wt. % nitrobenzene and $T_c=302.16$ K). Our value of T_c is, however, lower than the ones reported by Konecki[9] and by Lubezky and McIntosh.[6] The high value given by the latter group[6] ($T_c=303.4$ K) could be explained by the fact that their purification of commercial nitrobenzene only eliminated traces of water and that the presence of other impurities might then have modified the critical temperature.

The nitrobenzene and isooctane used in the measurements of the permittivity are identical to those used for the determination of the critical parameters. The experimental cell filled with the homogeneous nitrobenzene-isooctane mixture having the critical composition $X_c=51.7$ wt. % nitrobenzene is maintained initially at a temperature 7-K higher than T_c. The high-temperature limit of our measurements is based on the calibration of our cell which only went up to 313 K. The volume of the mixture is such that the meniscus appears at the level of the fourth capacitor from the bottom.

We measure the permittivity at different heights and the bulk permittivity as a function of the frequency between 0.1 and 100 kHz. The bulk permittivity is obtained by connecting all the capacitors in parallel (capacitors 2 to 11). The temperature is then lowered by steps to T_c and for each step, the same set of permittivity measurements is carried out. Far from T_c, temperature steps of 0.5 K are taken, each one requiring an equilibrium time of 30 minutes. In the range 1 mK $\leq T-T_c\leq0.8$ K, temperature steps are gradually reduced from 0.05 K to 1 mK. The equilibrium time ranges from one hour to over 24 hours as T_c is approached.

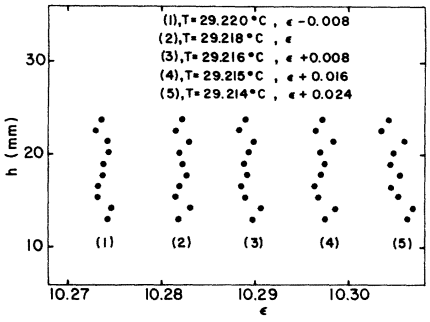

FIG. 2. The static permittivity ϵ as a function of height h for different temperatures T near the critical temperature T_c at a frequency of 100 kHz and for the critical composition.

IV. EXPERIMENTAL RESULTS

We have measured the static permittivity ϵ of the homogeneous nitrobenzene-isooctane mixture along its critical isochore ($X_c=51.7$ wt. % nitrobenzene) from 309.5 to 302.214 K; the latter being the limiting temperature at which we could perform capacitance measurements in the one-phase region. The ϵ data taken at a frequency of 100 kHz and covering the entire temperature range, are

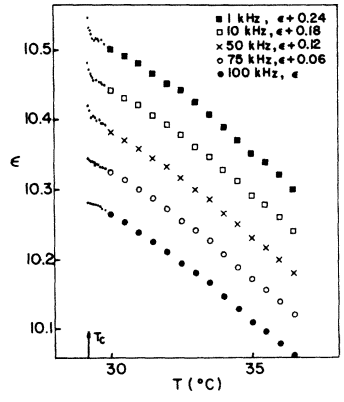

FIG. 3. The bulk static permittivity ϵ as a function of T above T_c for several frequencies and for the critical composition.

TABLE I. Experimental values for the static permittivity as a function of temperature for different heights in the sample.

T (°C)	σ (T)	14.00 mm	15.20 mm	16.40 mm	17.60 mm	18.80 mm	20.00 mm	21.20 mm	22.40 mm	23.60 mm	24.80 mm	Bulk
36.50	1×10^{-2}	10.0640	10.0652	10.0629	10.0635	10.0657	10.0642	10.0636	10.0643	10.0632	10.0639	10.0642
36.00		10.0817	10.0835	10.0811	10.0822	10.0838	10.0818	10.0817	10.0828	10.0821	10.0833	10.0803
35.50		10.0987	10.1003	10.0982	10.0995	10.1015	10.0990	10.0986	10.0997	10.0988	10.1013	10.0980
35.00		10.1151	10.1169	10.1140	10.1158	10.1175	10.1154	10.1148	10.1153	10.1151	10.1165	10.1143
34.50		10.1328	10.1339	10.1327	10.1332	10.1337	10.1324	10.1317	10.1328	10.1319	10.1330	10.1306
34.00		10.1492	10.1514	10.1484	10.1509	10.1523	10.1514	10.1507	10.1529	10.1518	10.1525	10.1487
33.50		10.1651	10.1665	10.1642	10.1647	10.1644	10.1672	10.1646	10.1662	10.1649	10.1664	10.1647
33.00		10.1793	10.1809	10.1777	10.1789	10.1792	10.1799	10.1794	10.1797	10.1788	10.1807	10.1804
32.50		10.1951	10.1964	10.1944	10.1958	10.1969	10.1961	10.1965	10.1973	10.1968	10.1970	10.1962
32.00		10.2095	10.2114	10.2088	10.2096	10.2108	10.2091	10.2113	10.2128	10.2122	10.2126	10.2120
31.50		10.2278	10.2296	10.2274	10.2284	10.2304	10.2286	10.2291	10.2319	10.2297	10.2311	10.2274
31.00		10.2423	10.2440	10.2412	10.2428	10.2433	10.2409	10.2423	10.2443	10.2422	10.2421	10.2418
30.50		10.2532	10.2550	10.2529	10.2538	10.2537	10.2536	10.2541	10.2557	10.2541	10.2536	10.2545
30.00		10.2676	10.2683	10.2661	10.2673	10.2675	10.2670	10.2668	10.2679	10.2667	10.2678	10.2678
29.800	5×10^{-3}	10.2721	10.2738	10.2723	10.2733	10.2743	10.2736	10.2733	10.2738	10.2713	10.2734	10.2717
29.700		10.2752	10.2756	10.2733	10.2743	10.2747	10.2741	10.2745	10.2753	10.2738	10.2748	10.2746
29.650		10.2756	10.2767	10.2750	10.2755	10.2758	10.2756	10.2760	10.2765	10.2761	10.2754	10.2760
29.600		10.2770	10.2776	10.2762	10.2765	10.2769	10.2773	10.2768	10.2778	10.2759	10.2766	10.2764
29.550		10.2779	10.2786	10.2768	10.2771	10.2780	10.2776	10.2774	10.2779	10.2766	10.2771	10.2776
29.500		10.2787	10.2792	10.2769	10.2777	10.2785	10.2782	10.2786	10.2794	10.2776	10.2780	10.2785
29.450		10.2798	10.2801	10.2780	10.2785	10.2790	10.2786	10.2791	10.2798	10.2789	10.2790	10.2793
29.400		10.2803	10.2812	10.2788	10.2789	10.2793	10.2790	10.2796	10.2806	10.2791	10.2795	10.2798
29.350		10.2810	10.2816	10.2789	10.2797	10.2790	10.2794	10.2789	10.2810	10.2793	10.2796	10.2802
29.300	1×10^{-3}	10.2808	10.2820	10.2790	10.2800	10.2803	10.2808	10.2796	10.2817	10.2797	10.2810	10.2804
29.250		10.2805	10.2824	10.2793	10.2802	10.2798	10.2801	10.2799	10.2820	10.2793	10.2797	10.2808
29.240		10.2813	10.2831	10.2790	10.2812	10.2796	10.2810	10.2808	10.2828	10.2801	10.2811	10.2809
29.230		10.2807	10.2831	10.2790	10.2803	10.2801	10.2796	10.2803	10.2824	10.2799	10.2807	10.2813
29.225		10.2822	10.2843	10.2796	10.2804	10.2810	10.2807	10.2813	10.2831	10.2806	10.2813	10.2815
29.220		10.2822	10.2826	10.2813	10.2816	10.2818	10.2819	10.2824	10.2821	10.2810	10.2816	10.2819
29.218	3×10^{-4}	10.2819	10.2832	10.2816	10.2820	10.2828	10.2823	10.2820	10.2830	10.2816	10.2821	10.2816
29.216		10.2818	10.2826	10.2809	10.2806	10.2811	10.2808	10.2813	10.2819	10.2803	10.2810	10.2815
29.215		10.2815	10.2826	10.2808	10.2804	10.2811	10.2814	10.2810	10.2824	10.2806	10.2812	10.2810
29.214		10.2823	10.2830	10.2815	10.2813	10.2815	10.2810	10.2813	10.2820	10.2802	10.2808	10.2813

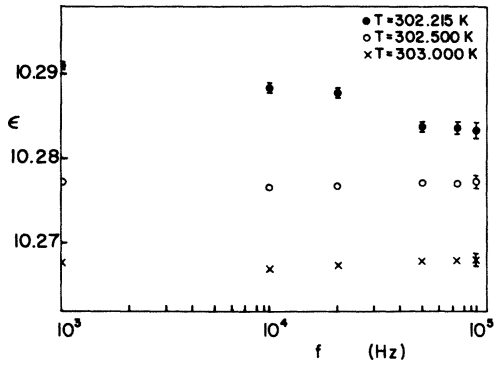

FIG. 4. Frequency dependence of the static permittivity for various temperatures near T_c.

compiled in Table I. The first two columns of Table I give the temperatures T and their standard deviations $\sigma(T)$ corresponding to the temperature steps indicated in Sec. III B. The ϵ values for the different heights which correspond to capacitor positions from 2 to 11, are given in columns 3—12. Column 13 gives the bulk permittivity values.

For temperatures close to the critical temperature T_c, we plot in Fig. 2 the ϵ data as a function of height h. Apart from the weak variations in the height dependence of ϵ which are probably due to small calibration errors of the capacitors; we observe no systematic deviation in $\epsilon(h)$ close to T_c. This indicates that in the measuring region, there are no composition gradients even at a few millidegrees above T_c.

In Fig. 3, we plot curves of the bulk permittivity as a function of temperature T for $f=1$, 10, 50, 75, and 100 kHz. Near T_c we observe sharp peaks in $\epsilon(T)$ for $f \leq 50$ kHz, confirming the results of Thoen *et al.*[10] The ϵ data as a function of frequency for various temperatures (Fig. 4) show near T_c, a low-frequency dispersion where the high frequency limit is attained at about 75 kHz. An enlarged graph of $\epsilon(T)$ near T_c at 75 and 100 kHz is presented in Fig. 5. It shows that within the experimental uncertainties, the temperature dependence of ϵ is consistent for the two frequencies. The ϵ data, corresponding to 100 kHz can certainly be taken to represent the critical behavior of the real static permittivity.

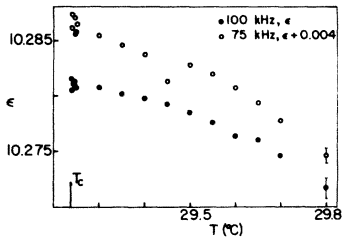

FIG. 5. Enlargement of a part of Fig. 2: temperature dependence of ϵ near T_c for 75 and 100 kHz.

V. ANALYSIS OF THE DATA

The purpose of this section is to analyze our experimental results at 100 kHz in terms of the theoretical expressions given in Sec. II. The ϵ data, which include 33 points covering a reduced temperature range $3.3\times10^{-6} \leq t \leq 2.4\times10^{-2}$, are fitted by the above mentioned expressions using the nonlinear least-squares program NL WOOD.[24] The data points are each weighted by the inverse of the variance $\mathrm{Var}(\epsilon)_i$ which increases for temperatures close to T_c. For the determination of $\mathrm{Var}(\epsilon)_i$, we have assumed two independent sources of errors: uncertainties in the determination of the static permittivity and uncertainties in temperature measurements. Using propagation of errors, we write the variance as

$$\mathrm{Var}(\epsilon)_i=\sigma(\epsilon)_i^2+\left[\frac{\partial\epsilon}{\partial T}\right]_i^2\sigma(T)_i^2 , \tag{3}$$

where $\sigma(\epsilon)_i$ and $\sigma(T)_i$ are the standard deviations of the static permittivity and temperature, respectively.

We use a reference standard capacitor (G. R. 1408.B) for the calibration of the internal capacitances of the ratio-transformer-bridge, and estimate $\sigma(\epsilon)_i$ to be 6×10^{-4} at a frequency of 100 kHz. This value of $\sigma(\epsilon)$ is well within the manufacturer's specifications which permit the determination of static permittivity at a frequency of 100 kHz with an accuracy better than 1.6×10^{-4}. The standard deviation $\sigma(T)_i$ of the temperature ranges from 1×10^{-2} to 3×10^{-4}, and the slope $(\partial\epsilon/\partial T)_i$ is estimated directly from the data. We perform several fits of the same data and the best one is determined by the minimum of the reduced χ^2 function, defined as

$$\chi_\nu^2=\frac{1}{N-p}\sum_i\frac{(\epsilon_i^{\mathrm{expt}}-\epsilon_i^{\mathrm{calc}})^2}{\mathrm{Var}(\epsilon)_i} , \tag{4}$$

where N is the number of experimental points and p is the number of adjustable parameters. Our complete data are fitted by Eq. (1) provided we add to it a linear term which reflects the behavior

of ϵ far from T_c

$$\epsilon=\epsilon_c+At^{\theta}+Bt \ . \tag{5}$$

Since the reduced temperature t does not exceed 2.4×10^{-2}, the polar contribution to ϵ due to the presence of nitrobenzene, expressed in t as $D/(1+t)$, can be written as $D(1-t)$. This contribution is then well taken into account in the linear term in Eq. (5).

On the basis of our experimental determination of ϵ, the critical temperature T_c must be between the temperature of the last data point (302.214 K) and 302.213 K at which we failed to make capacitance measurements even after three days of waiting. Because of the uncertainties in temperature measurements ($\pm3\times10^{-4}$), we fixed T_c at different values between 302.2143 and 302.2127 K, and fit the other parameters ϵ_c, A, B, and θ in Eq. (5). Results are given in lines 1–7 of Table II, and the χ^2_ν values are plotted as a function of T in Fig. 6. Uncertainties on the parameters correspond to one standard deviation. We note that the values of the adjustable parameters are weakly sensitive to the choice of T_c. A, B, and θ increase slightly with increasing T_c and ϵ_c is constant for all the fits ($\epsilon_c=10.2811$). This is probably due to the fact that A and B have opposite signs and the temperature range investigated for the determination of T_c is very narrow.

The best fits determined by the minimum of χ^2_ν (Table II and Fig. 6) corresponding to 302.2130

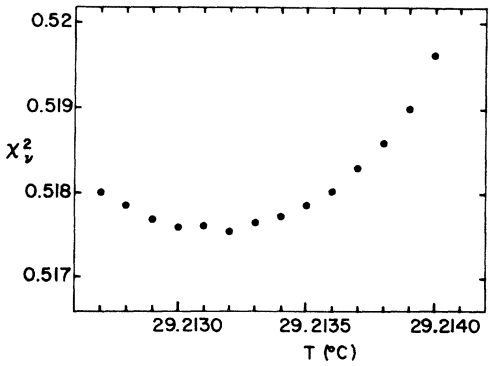

FIG. 6. Reduced chi-square as a function of temperature for the free fit of the data at 100 kHz to Eq. (5).

$K \le T_c \le 302.2134$ K, give for the critical exponent θ a value with relatively high uncertainty ($\theta=0.855\pm0.035$). To determine θ more precisely, we perform a series of fits by Eq. (5) in which θ is given different values, using for T_c the values previously determined. Results for the three adjustable parameters ϵ_c, A, and B, and χ^2_ν values for the fits are given in lines 8–13 of Table II. Uncertainties on A and B are substantially improved. Figure 7 giving the behavior of χ^2_ν as a function of θ for three temperatures, shows that the probable value of θ is 0.861, which is in agreement with the theoretical result deduced from the series expansion in a three-dimensional Ising model[25]

TABLE II. Values[a] for the parameters in Eq. (5) from different types of fits of the data.

Fit	T_c (°C)	ϵ_c	B	A	θ	χ^2_ν
1	(29.2140)	$10.2811\pm1.7\times10^{-4}$	-19.4 ± 2.7	6.1 ± 2.4	0.858 ± 0.035	0.5196
2	(29.2138)	$10.2811\pm1.7\times10^{-4}$	-19.4 ± 2.7	6.1 ± 2.3	0.857 ± 0.035	0.5186
3	(29.2136)	$10.2811\pm1.7\times10^{-4}$	-19.3 ± 2.6	6.0 ± 2.3	0.856 ± 0.035	0.5180
4	(29.2134)	$10.2811\pm1.7\times10^{-4}$	-19.3 ± 2.6	6.0 ± 2.3	0.856 ± 0.035	0.5177
5	(29.2132)	$10.2811\pm1.8\times10^{-4}$	-19.2 ± 2.6	5.9 ± 2.2	0.855 ± 0.035	0.5175
6	(29.2130)	$10.2811\pm1.8\times10^{-4}$	-19.1 ± 2.6	5.9 ± 2.2	0.854 ± 0.035	0.5176
7	(29.2128)	$10.2811\pm1.8\times10^{-4}$	-19.1 ± 2.5	5.8 ± 2.2	0.853 ± 0.035	0.5179
8	(29.2134)	$10.2811\pm1.3\times10^{-4}$	-19.77 ± 0.19	6.42 ± 0.11	(0.862)	0.5164
9	(29.2134)	$10.2811\pm1.3\times10^{-4}$	-19.44 ± 0.19	6.13 ± 0.11	(0.858)	0.5167
10	(29.2132)	$10.2811\pm1.3\times10^{-4}$	-19.78 ± 0.19	6.43 ± 0.11	(0.862)	0.5157
11	(29.2132)	$10.2811\pm1.3\times10^{-4}$	-19.45 ± 0.19	6.14 ± 0.11	(0.858)	0.5161
12	(29.2130)	$10.2811\pm1.3\times10^{-4}$	-19.78 ± 0.19	6.43 ± 0.11	(0.862)	0.5150
13	(29.2130)	$10.2811\pm1.3\times10^{-4}$	-19.45 ± 0.19	6.14 ± 0.11	(0.858)	0.5155
14	(29.2130)	$10.2811\pm1.3\times10^{-4}$	-20.90 ± 0.21	7.42 ± 0.13	(0.875)	0.5250
15	(29.2130)	$10.2812\pm1.3\times10^{-4}$	-22.77 ± 0.25	9.12 ± 0.16	(0.890)	0.5367

[a]Lines 1–7 correspond to the free fit of the parameters and lines 8–15 are obtained for fixed values of θ.

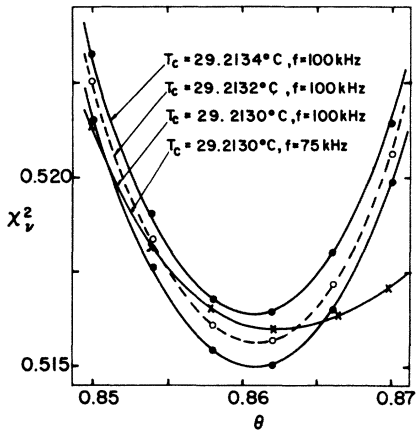

FIG. 7. Reduced chi-square as a function of fixed values of θ for the fit of the data (75 and 100 kHz) to Eq. (5) corresponding to three possible values of T_c.

(0.875 ± 0.020), but does not agree with the value obtained from renormalization group calculations[20] (0.890 ± 0.002). We give in lines 14 and 15 of Table II, the results from the fits when the theoretical values of θ are imposed (0.875 and 0.890). The χ^2_ν is substantially higher than for the best fit. The latter corresponds to $T_c=302.2130$ K and $\theta=0.861$, and the fitted parameters are

$$\epsilon_c=10.2811\pm1.3\times10^{-4},$$

$$B=-19.78\pm0.19,$$

$$A=6.43\pm0.11,$$

In the next step of the analysis, we introduce a singular correction to scaling term[18,19] which is included in the functional form given by Sengers *et al.*[18] and expressed by Eq. (2). In this set of analysis, we hold the correction exponent Δ fixed at the theoretical predicted value of 0.50,[20] and fit the five parameters A_0, A_1, B_1, C_1, and θ. Except A_0, the other parameters have larger uncertainties. Their values are quite close to those obtained previously. The χ^2_ν values are weakly lower than that of the best previous fits ($\chi^2_\nu\simeq0.514$), and the coefficient C_1 of the correction term is of the order of $-3.\times10^{-6}$. This indicates that adding a negative correction term to the equation does not improve the fit significantly, and that the contribution of the correction to scaling term can be considered as not essential to the model equation which describes our data.

We have also carried out a nonlinear least-squares analysis of ϵ as a function of temperature for our results at 75 kHz. Neglecting three outliers, the best fits obtained by minimizing the χ^2_ν function give parameter values which are consistent with those deduced from the 100-kHz analysis. They are for $T_c=302.2130$ K: $\epsilon_c=10.2816\pm4\times10^{-4}$, $A=6.2\pm3.5$, $B=-19.1\pm4.0$, and $\theta=0.869\pm0.049$. The reduced chi-square (χ^2_ν) as a function of the critical exponent θ for a temperature of 302.2130 K is given in Fig. 7. The lack of precision is probably due to the fact that 75 kHz is at the extreme limit of the dispersion region.

VI. CONCLUSION

In this paper, we have presented experimental evidence of the static permittivity anomaly near the critical temperature of the nitrobenzene-isooctane mixture. In order to determine unambiguously if the origin of this anomaly is different from that of the thermal expansion at the critical point, one has to measure both the static permittivity and the density for the same system.[18] This has been done by Jacobs and Greer[26] for the polystyrene-cyclohexane system, and they have observed small but detectable anomalous behavior of the static permittivity.

The critical behavior of ϵ was analyzed in terms of the existing theoretical expressions. We have found that the asymptotic form as expressed in Eq. (5) gives satisfactory fits to the data. The critical exponent θ as obtained from the free fit (0.855 ± 0.035) is in agreement with both theoretical values deduced from the field-theoretical approach[20] (0.890 ± 0.002) and from the series expansion in a three-dimensional Ising model[25] (0.875 ± 0.020). The more precise value of θ (0.861) obtained by reducing the number of adjustable parameters compares better with the series expansion value.

The functional form including correction-to-scaling terms[18] [Eq. (2)] was also tested. The quality of the fit is weakly improved and the contribution of the added term is not significant.

We have also studied the gravity effects in the mixture near T_c, using the variation of the static permittivity with height as an indication of the density profile in the field of gravity. We have found no gravity effects in the one-phase region near T_c within our experimental errors (the maximum spread in the static permittivity value as shown in Fig. 2 is of the order of 0.03% at the critical temperature).

ACKNOWLEDGMENTS

This work was supported by le Ministère de l'Education du Gouvernement du Québec and Natural Sciences and Engineering Research Council of Canada. We are indebted to Dr. Louis Marchildon and Dr. Jerzy Sochanski for helpful discussions during the preparation of this article. We are also grateful to Dr. J. Thoen for valuable suggestions.

[1]J. M. H. Levett Sengers, in *Experimental Thermodynamics,* edited by Le Neidre and B. Vodar (Butterworths, London, 1975), Vol. II B, Chap. 14.
[2]V. V. Semenchenko and M. Azimov, Zh. Fiz. Khim. 29, 1342 (1955).
[3]B. Ripley and R. McIntosh, Can. J. Chem. 39, 526 (1961).
[4]I. Lubezky and R. McIntosh, Can. J. Chem. 51, 545 (1973).
[5]M. Givon, L. Pelah, and V. Efron, Phys. Lett. A 48, 1 (1974).
[6]I. Lubezky and R. McIntosh, Can. J. Chem. 52, 3176 (1974).
[7]M. Hollecker, J. Goulon, J.-M. Thiebaut, and J.-L. Rivail, Chem. Phys. 11, 99 (1975).
[8]R. Halliwell, D. Hutchinson, and R. McIntosh, Can. J. Chem. 54, 1139 (1976).
[9]M. Konecki, Chem. Phys. Lett. 57, 90 (1978).
[10]J. Thoen, R. Kindt, and W. VanDael, Phys. Lett. A 76, 445 (1980).
[11]G. Stell and J. S. Hoye, Phys. Rev. Lett. 33, 1268 (1974).
[12]L. Mistura, J. Chem. Phys. 59, 4563 (1973).
[13]J. Goulon, J. L. Greffe, and D. W. Oxtoby, J. Chem. Phys. 70, 4742 (1979).
[14]D. W. Oxtoby and H. Metiu, Phys. Rev. Lett. 36, 1092 (1976).
[15]D. W. Oxtoby, Phys. Rev. A 15, 1251 (1977).
[16]K. W. Wagner, Arch. Elektrotech. (Berlin) 2, 371 (1914).
[17]C. J. F. Böttcher, Rec. Trav. Chim. 64, 47 (1945).
[18]J. V. Sengers, D. Bedeaux, P. Mazur, and S. C. Greer, Physica A (Utrecht) 104, 573 (1980).
[19]M. Ley-Koo and M. S. Green, Phys. Rev. A 16, 2483 (1977).
[20]J. C. LeGuillou and J. Zin-Justin, Phys. Rev. B 21, 3976 (1980).
[21]C. Hosticka and T. K. Bose, J. Chem. Phys. 60, 1318 (1974).
[22]J. A. Riddick and W. B. Bunger, in *Techniques of Chemistry,* edited by A. Weissberger (Wiley, New York, 1972), Vol. II, pp. 600–795.
[23]P. Debye and K. Kleboth, J. Chem. Phys. 42, 3155 (1965).
[24]C. Daniel and F. S. Wood, in *Fitting Equations to Data* (Wiley, New York, 1971).
[25]W. J. Camp, D. Saul, P. VanDyke, and M. Wortis, Phys. Rev. B 14, 3990 (1976).
[26]D. T. Jacobs and S. C. Greer, Phys. Rev. A 24, 2075 (1981).